Kinetic Mechanism of *Staphylococcus aureus* Sortase SrtA

Xinyi Huang,*,‡ Ann Aulabaugh,‡ Weidong Ding,‡ Bhupesh Kapoor,‡ Lefa Alksne,§ Keiko Tabei,|| and George Ellestad‡

Departments of Bioorganic/Enzymology, Infectious Diseases, and Analytical Chemistry, Wyeth Research, 401 North Middletown Road, Pearl River, New York 10965

Received March 10, 2003; Revised Manuscript Received July 2, 2003

ABSTRACT: *Staphylococcus aureus* sortase (SrtA) is a thiol transpeptidase. The enzyme catalyzes a cell wall sorting reaction in which a surface protein with a sorting signal containing a LPXTG motif is cleaved between the threonine and glycine residues. The resulting threonine carboxyl end of this protein is covalently attached to a pentaglycine cross-bridge of peptidoglycan. The transpeptidase activity of sortase has been demonstrated in in vitro reactions between a LPETG-containing peptide and triglycine. When a nucleophile is not available, sortase slowly hydrolyzes the LPETG peptide at the same site. In this study, we have analyzed the steady-state kinetics of these two types of reactions catalyzed by sortase. The kinetic results fully support a ping-pong mechanism in which a common acyl-enzyme intermediate is formed in transpeptidation and hydrolysis. However, each reaction has a distinct rate-limiting step: the formation of the acyl-enzyme in transpeptidation and the hydrolysis of the same acyl-enzyme in the hydrolysis reaction. We have also demonstrated in this study that the nucleophile binding site of *S. aureus* sortase SrtA is specific for diglycine. While S1′ and S2′ sites of the enzyme both prefer a glycine residue, the S1′ site is exclusively selective for glycine. Lengthening of the polyglycine acceptor nucleophile beyond diglycine does not further enhance the binding and catalysis.

The development of pathogens resistant to traditionally useful antibiotics, primarily because of the overprescription of these agents, has led to a crisis in the treatment of infectious diseases. This is especially true in hospital settings and has led to a search for new targets to screen for antimicrobials with novel modes of action. Most current clinically useful agents inhibit bacterial protein synthesis, bacterial cell wall formation, or nucleic acid synthesis. An emerging novel approach is to disrupt the anchoring of bacterial surface proteins critical for host−pathogen interactions. Gram-positive pathogenic bacteria display proteins on their surface, many of which have been shown to promote interactions between invading pathogens and host cells, resulting in bacterial attachment to host tissues and resistance to phagocytosis (*1*, *2*). A family of surface proteins, including protein A and clumping factors ClfA and ClfB from *Staphylococcus aureus*, contain a C-terminal sorting signal consisting of a LPXTG motif, a hydrophobic domain, and a positively charged tail (*3*, *4*). It has been suggested that, during anchoring, surface proteins are first initiated into the secretory pathway by means of an N-terminal leader peptide. The positively charged tail of the sorting signal functions to retain the proteins from committing further into the secretory pathway (*5*). The surface proteins are then subjected to the cell wall sorting, a reaction catalyzed by sortase.

S. aureus sortase (SrtA) is a 206 amino acid thiol transpeptidase with an N-terminal transmembrane anchor. Cys-184 and His-120 of *S. aureus* sortase are essential for the enzymatic activity and have been suggested to form a thiolate−imidazolium ion pair for catalysis (*6*). *S. aureus* sortase catalyzes a transpeptidation reaction in which a surface protein with a LPXTG sorting signal is cleaved between the threonine and glycine residues. Then the carboxyl group of the threonine is amide linked to the amino group of a pentaglycine cross-bridge of the cell membrane-attached peptidoglycan (*7*−*10*). Through this reaction, surface proteins are covalently anchored to the bacterial cell wall.

Sortase likely plays a universal role in the virulence of Gram-positive bacteria. Surface proteins containing the LPXTG sorting signal have been located in all pathogenic Gram-positive bacteria examined to date (*2*, *11*). Schneewind and co-workers have elegantly demonstrated that sortase is essential for the functional assembly of cell surface expressed virulence factors and pathogenesis of *S. aureus* infections (*12*, *13*). Bierne et al. have shown that inactivation of the sortase SrtA gene in *Listeria monocytogenes* similarly inhibits anchoring of surface proteins and impairs virulence (*14*). Therefore, inhibition of sortase activity may provide a novel approach for the treatment of infections caused by Gram-positive bacteria, complementing current exclusive reliance on conventional antibiotics. Sortase inhibitors may act as anti-infective agents, disrupting the pathogenesis of bacterial infections without affecting microbial viability. This type of treatment may result in decreased drug resistance.

Despite the clinical significance of sortase, the kinetics of sortase has not been thoroughly investigated. In addition to the transpeptidation reaction, sortase also catalyzes the hydrolysis reaction in vitro in the absence of a nucleophile

* To whom correspondence should be addressed. Phone: (845) 602-3374. Fax: (845) 602-5687. E-mail: huangx@wyeth.com.
‡ Department of Bioorganic/Enzymology, Wyeth Research.
§ Department of Infectious Diseases, Wyeth Research.
|| Department of Analytical Chemistry, Wyeth Research.

10.1021/bi034391g CCC: $25.00
Published on Web 09/05/2003

Scheme 1

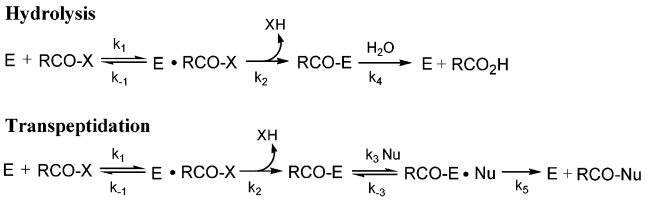

(*6*, *15*). Scheme 1 shows minimal models for the transpeptidation and hydrolysis reaction. In this paper, we describe steady-state kinetic analysis of both transpeptidation and hydrolysis reactions. The results fully support the formation of a common acyl-enzyme intermediate in both reactions as shown in Scheme 1. However, each reaction has a distinct rate-limiting step. We have also probed the specificity of the nucleophilic polyglycine peptide. Our study demonstrates that the nucleophile binding site is specific for diglycine. While S1′ and S2′ sites both prefer a glycine residue, the S1′ site is exclusively selective for glycine.

MATERIALS AND METHODS

Materials. The enzyme used in this study was a soluble His-tagged construct of *S. aureus* sortase (SrtA) that lacks the N-terminal transmembrane region (Δ25). The enzyme was supplied by SIGA Pharmaceuticals. This sortase construct is identical to a previously published construct SrtΔN (*8*). FRET assay peptide substrate Abz-LPETG-Dnp[1] and hydrolysis products Abz-LPET-OH and NH_2-G-Dnp were custom synthesized by AnaSpec. Peptides Gly, Gly-NH_2, GlyGly, GlyGlyGly, GlyGlyHis, GlyGlyLeu, GlyGlyGlyGly, GlyGlyGlyGlyGly, AlaGly, ValGly, GlyAla, GlyVal, AcetylGly, and AlaAla were purchased from Sigma or Aldrich.

Kinetic Measurements. A FRET assay was used to monitor the in vitro activity of sortase. In this activity assay, Abz-LPETG-Dnp, a fluorescently self-quenched peptide, now replaced the surface protein substrate containing a LPETG sorting signal, and triglycine replaced the pentaglycine cross-bridge of peptidoglycan as the new nucleophile. When Abz-LPETG-Dnp is cleaved by sortase, the fluorophore Abz group is separated from the quencher Dnp group, resulting in an enhanced fluorescence signal. Mass spectrometry confirmed that the enzyme catalyzed the formation of Abz-LPET-GGG, the transpeptidation product, in the presence of triglycine and the formation of Abz-LPET-OH in the absence of triglycine. This FRET assay using Abz-LPETG-Dnp as a substrate has been described previously (*6*). The reaction was performed in the assay buffer containing 20 mM HEPES, pH 7.5, and 5 mM $CaCl_2$. In a typical kinetic measurement, the reaction in the absence or the presence of triglycine was started by the addition of sortase. The increase in fluorescence was then continuously monitored at room temperature at λ_{em} 420 nm and λ_{ex} 335 nm for 60 min on a SpectraMax Gemini XS fluorescence plate reader. The velocities determined from the progress curves (the steady-state rates in the case of biphasic curves) at various substrate concentrations were fit to eq 1 to determine the apparent K_m and k_{cat} values.

$$v = \frac{k_{cat}ES}{S + K_m} \tag{1}$$

Kinetic Equations. On the basis of models for the hydrolysis and transpeptidation in Scheme 1, kinetic equations delineating the relationship between observed kinetic constants and microscopic kinetic constants (eqs 2−7) can be derived using the net rate constant method developed by Cleland (*16*) (see Appendix for derivation). Equations 2 and 3 describe the hydrolysis reaction in the absence of the second substrate. K_{mPep} in eq 2 represents the peptide Michaelis−Menten constant in the overall hydrolysis reaction. Equations 4 and 5 describe the transpeptidation reaction when the concentration of the nucleophile is fixed at S_2. If the concentration of the peptide is fixed at S_1, then the transpeptidation reaction can be described by eqs 6 and 7. In eqs 4−7, $K_{mPep,app}$, $K_{mNu,app}$, $k_{catPep,app}$, and $k_{catNu,app}$ represent experimentally determined apparent kinetic constants, while $K_m^\circ{}_{Pep}$ and $K_m^\circ{}_{Nu}$ are defined respectively as the peptide Michaelis−Menten constant $[(k_2 + k_{-1})/k_1]$ for the *first* half-reaction of the overall transpeptidation reaction and the nucleophile Michaelis−Menten constant $[(k_5 + k_{-3})/k_3]$ for the *second* half-reaction of the overall transpeptidation reaction. By virtue of the definition of $K_m^\circ{}_{Pep}$, the hydrolysis and transpeptidation reaction as depicted in Scheme 1 share the same $K_m^\circ{}_{Pep}$ value.

When both the peptide concentration (S_1) and nucleophile concentration (S_2) were varied in the transpeptidation reaction, the data were fit to eq 8, which describes the ping-pong bi-bi kinetic mechanism (*20*). K_{mPep} and K_{mNu} in eq 8 represent Michaelis−Menten constants in the overall transpeptidation reaction. K_{mPep} is related to the above-defined $K_m^\circ{}_{Pep}$ by a factor of $k_5/(k_2 + k_5)$, while K_{mNu} is related to $K_m^\circ{}_{Nu}$ by a factor of $k_2/(k_2 + k_5)$. When $K_{mPep,app}$ and $K_{mNu,app}$ in eqs 4 and 6 are determined in the presence of a fixed saturating concentration of the second substrate, they become respectively equal to K_{mPep} and K_{mNu}, the Michaelis constants in eq 8 (see Appendix).

$$K_{mPep} = K_m^\circ{}_{Pep}\frac{k_4}{k_2 + k_4} \tag{2}$$

$$k_{cat} = \frac{k_2k_4}{k_2 + k_4} \tag{3}$$

$$K_{mPep,app} = K_m^\circ{}_{Pep}\frac{\dfrac{k_5}{1 + K_m^\circ{}_{Nu}/S_2}}{k_2 + \dfrac{k_5}{1 + K_m^\circ{}_{Nu}/S_2}} \tag{4}$$

$$k_{catPep,app} = k_2\frac{\dfrac{k_5}{1 + K_m^\circ{}_{Nu}/S_2}}{k_2 + \dfrac{k_5}{1 + K_m^\circ{}_{Nu}/S_2}} \tag{5}$$

[1] Abbreviations: Abz, *o*-aminobenzoyl; Dnp, 2,4-dinitrophenyl; DTT, dithiothreitol; BME, β-mercaptoethanol; Edans, 5-[(2-aminoethyl)-amino]naphthalene-1-sulfonic acid; Dabcyl, 4-[[4-(dimethylamino)-phenyl]azo]benzoic acid; FRET, fluorescence resonance energy transfer; ESIMS, electrospray ionization mass spectrometry; TFA, trifluoroacetic acid.

$$K_{mNu,app} = K_m^{\circ}{}_{Nu} \frac{\dfrac{k_2}{1 + K_m^{\circ}{}_{Pep}/S_1}}{k_5 + \dfrac{k_2}{1 + K_m^{\circ}{}_{Pep}/S_1}} \quad (6)$$

$$k_{catNu,app} = k_5 \frac{\dfrac{k_2}{1 + K_m^{\circ}{}_{Pep}/S_1}}{k_5 + \dfrac{k_2}{1 + K_m^{\circ}{}_{Pep}/S_1}} \quad (7)$$

$$v = \frac{V_m S_1 S_2}{K_{mNu} S_1 + K_{mPep} S_2 + S_1 S_2} \quad (8)$$

If the k_4 step is a rate-determining step in the hydrolysis reaction (Scheme 1), then burst kinetics is expected (*17*). This type of biphasic progress curves can be described by eq 9, where π is the amplitude of burst and V_s is the steady-state velocity.

$$P = \pi[1 - \exp(-k_{obs}t)] + V_s t \quad (9)$$

RESULTS AND DISCUSSION

Previous studies have shown that sortase catalyzes an in vitro transpeptidation reaction between a LPETG-containing peptide and triglycine (*6*, *15*). In the absence of an acceptor nucleophile, sortase catalyzes the hydrolysis of this peptide. In the current study, both types of sortase activities were monitored via a fluorogenic substrate Abz-LPETG-Dnp. To correlate the fluorescence signal (RFU) with the concentration, the standard curves of Abz-LPET-OH in the absence and presence of an equal concentration of NH_2-G-Dnp were collected (Figure 1). The presence of NH_2-G-Dnp clearly decreased the fluorescence of Abz-LPET-OH. However, the quenching effect was minimal when the quencher concentration was below 20 μM. The linear segment of the fluorophore standard curve generated a conversion ratio of 144 RFU/μM Abz-LPET-OH. Separately, the exhaustive hydrolysis of 2 μM Abz-LPETG-Dnp by 100 μM sortase yielded a RFU of 224 or a conversion ratio of 112 RFU/μM Abz-LPET-OH. This conversion ratio is close to the value obtained from the standard curve. In the following discussion, parameters containing RFU have been converted to micromolar.

Hydrolysis of Abz-LPETG-Dnp. Sortase catalyzes the hydrolysis of peptide Abz-LPETG-Dnp in the absence of a nucleophile. Hydrolysis products Abz-LPET-OH and NH_2-G-Dnp have been identified by HPLC and mass spectrometry (*6*). Figure 2A shows progress curves of the sortase-catalyzed hydrolysis reaction at various Abz-LPETG-Dnp concentrations. Each progress curve is clearly biphasic, and the burst amplitude (π) increases with the peptide concentration. For each progress curve, the amount of fluorescent product (after conversion from RFU to concentration) was less than 10% of the initial substrate concentration. Since both the acyl-enzyme and the product Abz-LPET-OH (see Scheme 1) were fluorescent, the burst amplitude and k_{obs} were too complex for the pre-steady-state analysis. However, the rate at steady state is solely contributed by the production of Abz-LPET-OH. The steady-state rate (V_s) was determined by fitting the data in Figure 2A to eq 9. The K_m for Abz-LPETG-Dnp in the hydrolysis reaction was determined to be 20 $\pm$ 4 μM from fitting the V_s data to eq 1 (Figure 2B). The k_{cat} value was 0.0073 $\pm$ 0.0006 min^{-1}. The second-order rate constant for hydrolysis of Abz-LPETG-Dnp was 0.37 mM^{-1} min^{-1}. The observed burst kinetics was consistent with a two-step kinetic scheme in which the acyl-enzyme accumulated at steady state and its turnover was a rate-limiting step in the overall hydrolysis reaction. Under these conditions, according to eq 2 the observed K_m of 20 μM for the overall hydrolysis reaction is a fraction of $K_m^{\circ}{}_{Pep}$, the peptide Michaelis−Menten constant for the *first* half-reaction. Electrospray ionization mass spectrometry confirmed the accumulation of the acyl-enzyme in the sortase reaction in the absence of a nucleophile. Figure 3 showed the ESIMS data of

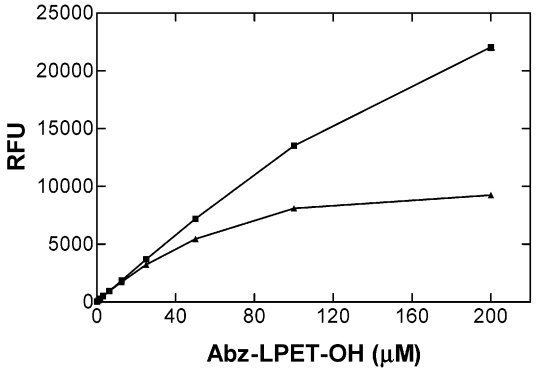

FIGURE 1: Standard curves of Abz-LPET-OH in the presence (▲) and absence (■) of an equal concentration of NH_2-G-Dnp. The fluorescence intensity was measured at λ_{ex} 335 nm and λ_{em} 420 nm.

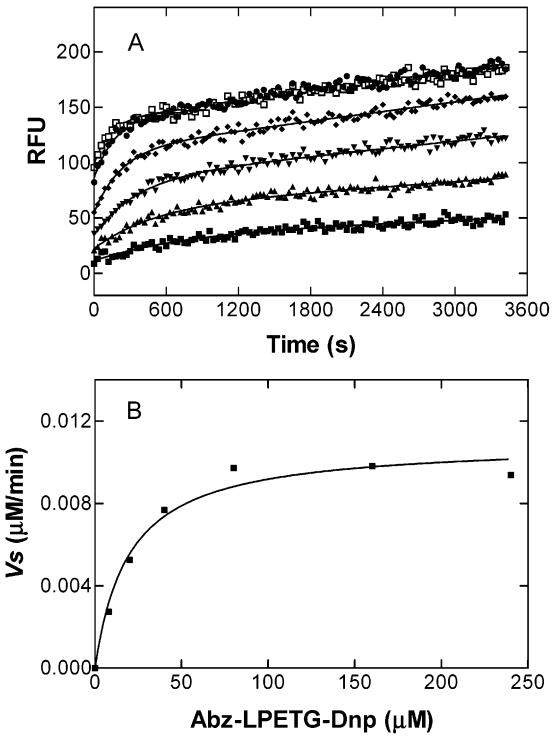

FIGURE 2: (A) Progress curves of the hydrolysis of Abz-LPETG-Dnp by sortase. The reaction solutions contained various concentrations of Abz-LPETG-Dnp [8 (■), 20 (▲), 40 (▼), 80 (◆), 160 (●), and 240 μM (□)] and 1.5 μM sortase. (B) Steady-state rate plotted against the concentration of Abz-LPETG-Dnp. Nonlinear regression to eq 1 generated a K_m of 20 $\pm$ 4 μM and a k_{cat} of 0.0073 $\pm$ 0.0006 min^{-1}.

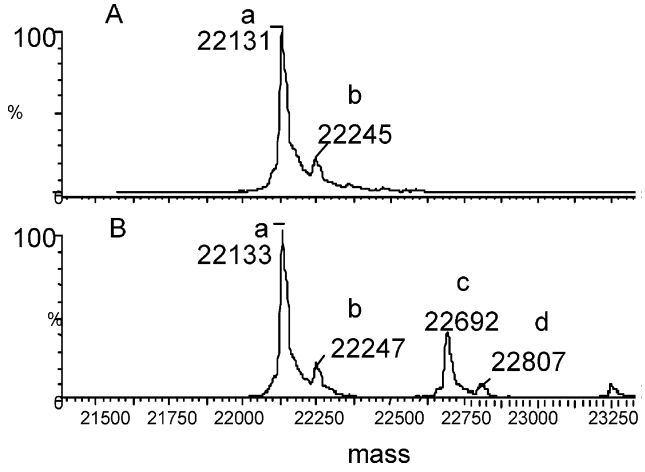

FIGURE 3: Electrospray ionization mass spectrometry of sortase reactions quenched by 1% final TFA. ESIMS was acquired using a Micromas Q-ToF mass spectrometer equipped with a nanoelectrospray source. (A) The sortase only control (10 μM) displayed mass peaks of 22131 (a) and 22245 (b), corresponding respectively to sortase and sortase plus TFA. (B) The sortase hydrolysis reaction that contained 10 μM sortase and 100 μM Abz-LPETG-Dnp was quenched after 90 min at room temperature. In addition to the two free enzyme mass peaks [22133 (a) and 22247 (b)], the mass spectrometry contained mass peaks of 22692 (c) and 22807 (d) and a minor higher mass peak. Masses of 22692 and 22807 match respectively to masses of the acyl-enzyme and the acyl-enzyme plus TFA. The minor peak could not be positively assigned.

sortase reactions quenched by a 1% final concentration of trifluoroacetic acid. The enzyme control shown in panel A contained mass peaks of 22131 and 22245, corresponding respectively to masses of sortase (22134, the Δ25 construct used in this study) and sortase plus TFA (22248). The hydrolysis reaction shown in panel B contained an additional set of mass peaks at 22692 and 22807, which match respectively the masses of the acyl-enzyme (22693) and the acyl-enzyme plus TFA (22807). A minor higher mass peak in panel B could not be positively assigned.

Sortase Transpeptidation Reaction between Abz-LPETG-Dnp and Triglycine. Figure 4A shows a set of progress curves at various Abz-LPETG-Dnp concentrations when the triglycine concentration was fixed at 3 mM (at saturation; see below). Each progress curve is essentially monophasic, suggesting that the rate-limiting step has switched to the k_2 step in the presence of triglycine (Scheme 1). The kinetic behavior is consistent with the lack of steady-state accumulation of the acyl-enzyme intermediate as observed in a separate mass spectrometry experiment. The only ESIMS mass peaks detected were 22131 and 22245, corresponding respectively to the masses of sortase and sortase plus TFA (data not shown; similar to Figure 3A). For each progress curve in Figure 4A, the substrate turnover was less than 10%. Thus the rate obtained represented the initial rate. Fitting of the rate vs Abz-LPETG-Dnp concentration to eq 1 generated a $K_{m,app}$ of 141 $\pm$ 19 μM and a k_{cat} value of 0.096 $\pm$ 0.007 min^{-1} for the transpeptidation reaction (Figure 4B). Since the $K_{m,app}$ for the peptide was determined in the presence of saturating triglycine, it now became K_{mPep}, the peptide Michaelis constant for the overall transpeptidation reaction (see Materials and Methods and Appendix). In addition, due to a rate-limiting acylation step (k_2) in the transpeptidation reaction, according to eq 4 $K_m^{\circ}{}_{Pep}$, the peptide K_m value for

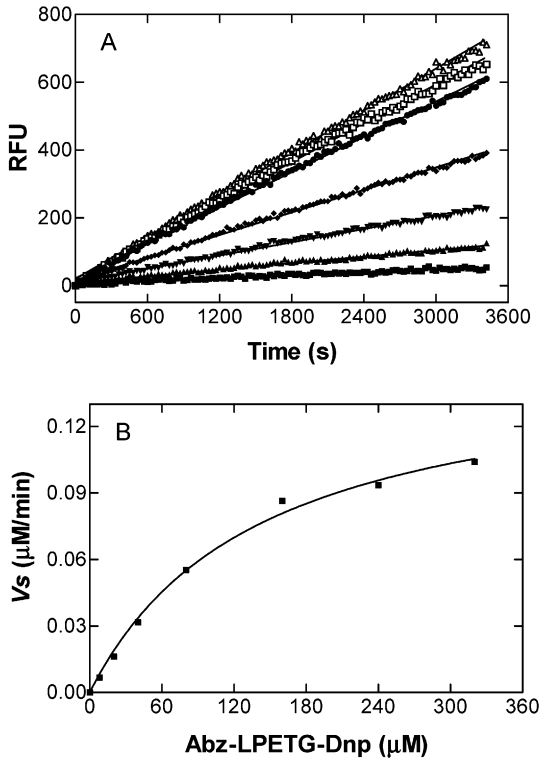

FIGURE 4: (A) Progress curves of the transpeptidation reaction at various concentrations of Abz-LPETG-Dnp. The reaction solutions contained various concentrations of Abz-LPETG-Dnp [8 (■), 20 (▲), 40 (▼), 80 (◆), 160 (●), 240 (□), and 320 μM (△)], 3 mM triglycine, and 1.5 μM sortase. (B) Steady-state rate plotted against the concentration of Abz-LPETG-Dnp. Nonlinear regression to eq 1 generated a $K_{m,app}$ of 141 $\pm$ 19 μM and a k_{cat} of 0.096 $\pm$ 0.007 min^{-1}.

the first half-reaction, is approximately the same as $K_{mPep,app}$ when the concentration of triglycine is saturating. The k_{cat}/K_{mPep} value for the transpeptidation reaction is 0.68 mM^{-1} min^{-1}. This second-order rate constant is similar to the corresponding rate constant for hydrolysis of Abz-LPETG-Dnp, again suggesting common reaction intermediates up to the acyl-enzyme intermediate before the binding of the second substrate in these two reaction pathways as shown in Scheme 1.

Figure 5A shows progress curves at various triglycine concentrations when the Abz-LPETG-Dnp concentration was fixed at 200 μM. Consistent with a change in the rate-determining step, the progress curves change from biphasic curves to linear curves with increasing concentration of triglycine. Fitting of the steady-state rate data to eq 1 yielded a $K_{m,app}$ of 24 $\pm$ 4 μM for triglycine (Figure 5B). Since the Abz-LPETG-Dnp concentration was 1.4 $\times$ K_m, according to eq 6 this $K_{m,app}$ for triglycine may underestimate the K_m value for triglycine in the overall transpeptidation reaction (see Materials and Methods for a definition of K_{mNu}) by about 2-fold.

Kinetic Mechanism of Sortase. To lend additional support to the proposed ping-pong mechanism for the sortase transpeptidation reaction, as outlined in Scheme 1, the concentrations of Abz-LPETG-Dnp and triglycine were both varied in the sortase assay. Figure 6 shows double reciprocal plots of the velocity versus the Abz-LPETG-Dnp concentration at three triglycine concentrations. Global fit of data in Figure 6 to eq 8 resulted in a parallel line pattern and a K_m

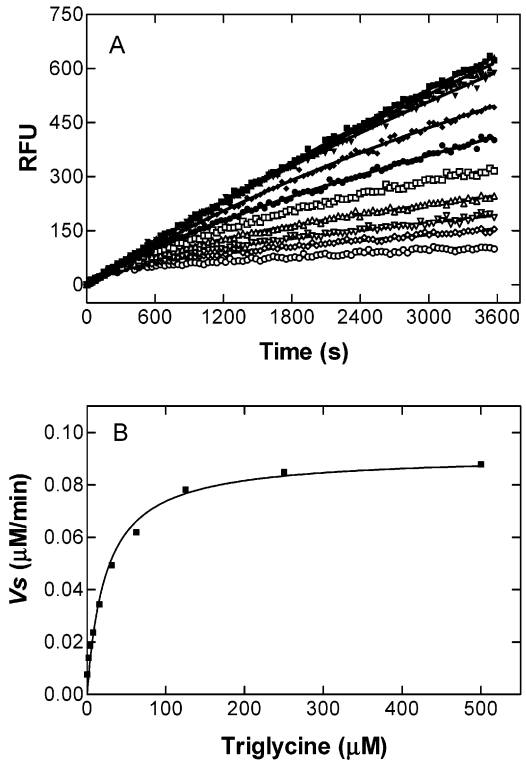

FIGURE 5: (A) Progress curves of the transpeptidation reaction at various concentrations of triglycine. The assays contained various concentrations of triglycine [0 (○), 2 (◇), 3.9 (▽), 7.8 (△), 15.6 (□), 31.3 (●), 62.5 (◆), 125 (▼), 250 (▲), and 500 (■) μM], 200 μM Abz-LPETG-Dnp, and 1.5 μM sortase. (B) Steady-state rate plotted against the concentration of triglycine. Nonlinear regression to eq 1 generated a $K_{m,app}$ of 24 ± 4 μM and a $k_{cat,app}$ of 0.061 ± 0.002 min^{-1}.

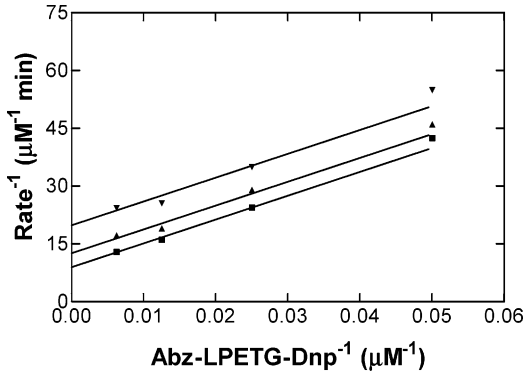

FIGURE 6: Double reciprocal plots of the velocity versus the Abz-LPETG-Dnp concentration at three fixed triglycine concentrations. The assays contained various concentrations of triglycine [15 (▼), 30 (▲), and 60 (■) μM], various concentrations of Abz-LPETG-Dnp (20, 40, 80, and 160 μM), and 2 μM sortase. The data were fit to eq 8.

of 117 ± 17 μM for Abz-LPETG-Dnp and a K_m of 41 ± 7 μM for triglycine. This result clearly suggests that the transpeptidation reaction catalyzed by sortase follows a ping-pong kinetic mechanism in which triglycine only binds to the enzyme when the acyl-enzyme is already formed. The K_m value for Abz-LPETG-Dnp obtained from this global fit is similar to the earlier determined peptide K_m value (141 μM). The K_m for triglycine determined from this global fit (41 μM) matches an earlier K_m estimate of 48 μM. As discussed in Materials and Methods, the K_m for triglycine represents the Michaelis−Menten constant for the overall

Scheme 2

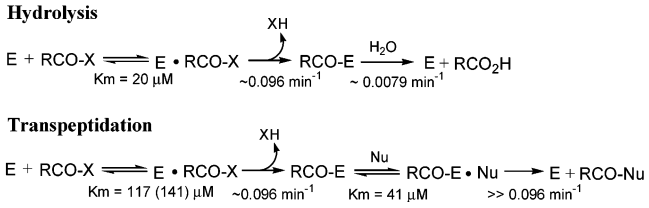

transpeptidation reaction, *not* for the second half of the reaction.

However, the parallel line pattern by itself does not rule out either an ordered bi-bi mechanism with a small K_{iPep} or a Theorell−Chance mechanism with a small K_{iPep}. A Theorell−Chance mechanism can be considered as a special case of ordered bi-bi in which the ternary complexes do not appreciably accumulate. In both ping-pong and Theorell−Chance mechanisms there is an extra $K_{iPep}K_{mNuc}$ term in the denominator of eq 8. Two hallmark features of a ping-pong mechanism are the chemical reaction between the enzyme and one substrate and the release of one product, both preceding the binding of the second substrate. In an ordered bi-bi mechanism, both the chemical reaction and the product release do not occur before the formation of the enzyme−substrate ternary complex. Indeed, both the acyl-enzyme and the product NH_2-G-Dnp were observed in the sortase hydrolysis reaction, the partial sortase reaction in the absence of the second substrate triglycine. In addition, the initial segment of progress curves of the hydrolysis reaction overlaps that of the transpeptidation reaction (see Figure 5A), and the overall transpeptidation reaction has a second-order rate constant virtually identical to the rate constant for the overall hydrolysis. These observations suggest common reaction intermediates up to the acyl-enzyme intermediate before the binding of the second substrate in these two reaction pathways as shown in Scheme 1. The above results in combination with the parallel line pattern rule out both ordered bi-bi and Theorell−Chance as the mechanism for the sortase transpeptidation reaction.

Microscopic kinetic parameters for both hydrolysis and transpeptidation in Scheme 1 can be estimated from experimentally determined steady-state kinetic values. Since the acylation step of the transpeptidation reaction is the rate-limiting step, based upon eq 5, the k_{cat} value for transpeptidation can be used as an approximation of k_2. For the hydrolysis of Abz-LPETG-Dnp, k_2 is the same as in transpeptidation (see Scheme 1), and k_4 can be calculated by eq 3 from k_2 and the k_{cat} for hydrolysis. This yields a k_4 of 0.0079 min^{-1}. Using these estimated constants, one is able to predict K_{mPep} for the overall hydrolysis reaction using eq 2:

$$K_{mPep} = K_m^{\circ}{}_{Pep}k_4/(k_4 + k_2) = 11\ \mu M$$

This value is close to the experimental value (20 μM). The overall kinetic parameters are summarized as in Scheme 2.

Recently, Schneewind and co-workers published preliminary results on the kinetics of sortase using a self-quenched peptide Dabcyl-QALPETGEE-Edans that has a Dabcyl group as the quencher and an Edans group as the fluorophore (*15*). Except for an unexplained lag, linear progress curves up to 30 min were reported for both hydrolysis and transpeptidation reactions. The rate of transpeptidation calculated from the

linear segment in the presence of 5 mM glycine, diglycine, and triglycine was respectively 6%, 10%, and 58% faster than hydrolysis (*15*). We are unable to explain these results except by pointing out that the concentration of sortase in the assay was nearly the same as the concentration of the substrate Dabcyl-QALPETGEE-Edans. On the basis of these small increases in the peptide cleavage in the presence of glycine, diglycine, and triglycine, the authors suggested that the nucleophilic attack of the acyl-enzyme intermediate by the pentaglycine cross-bridge of peptidoglycan is the rate-limiting step of surface protein anchoring (*15*). This is different from our results that showed the acylation step was rate-determining in transpeptidation in vitro. While we think it is unlikely that two similar LPETG peptides can result in a change in the rate-limiting step, the nature of the observed kinetic behavior of Dabcyl-QALPETGEE-Edans remains to be elucidated.

Schneewind and co-workers also examined the sortase hydrolysis reaction employing Abz-LPETG-Dnp as a substrate (*6*). The apparent K_m for this peptide was determined to be 116 μM, higher than a K_{mPep} value of 20 μM from our study. Because the hydrolysis reaction in their study was monitored for only 100 s, biphasic kinetics was not observed. Our study has shown that progress curves of the hydrolysis reaction are biphasic. Clearly, analysis of only the first 100 s of the progress curve, in which only acylation occurs, will result in approximate parameters for the acylation step but not for the entire hydrolysis reaction. Therefore, the apparent K_m for the peptide determined in their study (116 μM) reflects the K_m for the *first* half of the reaction, which is in agreement with the peptide $K_m^\circ{}_{Pep}$ as determined in our study ($\sim$141 μM). These authors also reported a k_{cat} value of 0.57 s^{-1} for the hydrolysis reaction. It is now clear that this value is not the k_{cat} for the hydrolysis reaction, rather a rough estimate for the acylation step (k_2, Schemes 1 and 2). However, this number is still >300-fold higher than the k_2 value determined from our study, even though the assay conditions and protein construct are apparently the same. Considering sortase is very slow in in vitro reactions, a value of 0.57 s^{-1} seems high (*6*, *15*).

Probing the Specificity of Nucleophilic Polyglycine Peptide. *S. aureus* sortase attaches surface proteins covalently to the pentaglycine cross-bridge of peptidoglycan. Although the solution NMR structure of sortase has been solved in the absence of substrate (*18*), the structure sheds no light on the binding of polyglycine to the enzyme. Both our study and literature studies (*6*, *15*) have demonstrated that triglycine can act as a nucleophile for in vitro transpeptidation. The possibility of an even shorter polyglycine, non-glycine peptide, or non-peptide nucleophile working as a nucleophile is not clear. Elucidation of the nucleophile specificity might also help to identify the nucleophile binding site in the sortase structure.

A number of polyglycine-related peptides and non-peptide nucleophiles were evaluated for the ability to react with the acyl-enzyme (Abz-LPET-sortase). The results are summarized in Table 1. Among nucleophiles tested, all peptides containing N-terminal diglycine (GlyGlyGlyGly, GlyGlyGly, GlyGlyHis, GlyGlyLeu, and GlyGly) can act as a nucleophile in the sortase transpeptidation reaction. These peptides have almost identical kinetic constants, suggesting that the acylation step is the rate-determining step in all cases. These

Table 1: Possible Nucleophiles for the Sortase Transpeptidation Reaction[a]

nucleophile	$K_{m,app}$ (μM)	V_m (μM/min)
GlyGlyGlyGlyGly	not tested	
GlyGlyGlyGly	16 $\pm$ 2	0.11 $\pm$ 0.01
GlyGlyGly	24 $\pm$ 4	0.09 $\pm$ 0.01
GlyGlyHis	20 $\pm$ 2	0.11 $\pm$ 0.01
GlyGlyLeu	35 $\pm$ 5	0.10 $\pm$ 0.01
GlyGly	30 $\pm$ 4	0.10 $\pm$ 0.01
GlyAla	127 $\pm$ 22	0.10 $\pm$ 0.01
GlyVal	208 $\pm$ 28	0.09 $\pm$ 0.01
AlaGly	NS[b]	
ValGly	NS[b]	
AlaAla	NS[b]	
Gly	NS[b]	
Ac-Gly	NS[b]	
Gly-NH_2	23 $\pm$ 2	0.12 $\pm$ 0.01
DTT	NS[c]	
BME	NS[c]	

[a] The reactions contained various concentrations of the nucleophile, 200 μM Abz-LPETG-Dnp, and 1.5 μM sortase. The velocities determined from the progress curves (the steady-state rates in the case of biphasic curves) at various nucleophile concentrations were fit to eq 1 to obtain the apparent K_m and V_m values. [b] No stimulation over the rate of the hydrolysis reaction up to 5 mM. [c] No stimulation over the rate of the hydrolysis reaction up to 10 mM.

results suggest that the third, fourth, and fifth glycine residues of the pentaglycine cross-bridge of peptidoglycan do not contribute significantly to the binding and catalysis. When the first glycine of diglycine is substituted, as in AlaGly and ValGly, no stimulation of deacylation is observed. Interestingly, when the second glycine of diglycine is replaced, as in GlyAla and GlyVal, these peptide nucleophiles still react with the acyl-enzyme. However, the $K_{m,app}$ values are elevated 5−10-fold. Therefore, while S1′ and S2′ sites of sortase both prefer a glycine residue, the S1′ site is exclusively selective for glycine.

Glycinamide can also act as the second substrate in transpeptidation. Amazingly, the kinetic constants are still very similar to that of triglycine. However, glycine does not react with the acyl-enzyme and neither does the reducing agent DTT or BME. Since glycine, DTT, and BME do not react with the acyl-enzyme, the amide bond between the first and second glycine must be critically involved in the binding of the nucleophile to sortase. In addition, a diglycine analogue without the N-terminal amino group (Ac-Gly) does not stimulate the deacylation. This is expected since Ac-Gly lacks the nucleophilic amino group. In all cases when a saturating concentration of nucleophiles is present in the transpeptidation reaction, the progress curve becomes essentially monophasic, and the acylation step most likely remains the rate-determining step. The rate of the deacylation step is fast and may vary from one nucleophile to the next.

In an earlier publication by Ton-That et al., it was shown that the rate of cleavage of a LPETG peptide was enhanced in the presence of 5 mM glycine, diglycine, and triglycine by 6%, 10%, and 58%, respectively (*15*). We have demonstrated in this paper the fundamental differences between glycine and diglycine (or triglycine). Diglycine and triglycine both enhance the rate of cleavage by more than 10-fold. However, glycine does not work as a nucleophile in transpeptidation.

Physiological Implications. The preference of sortase for diglycine as a nucleophile suggests that only the first two

glycine residues of the pentaglycine segment of lipid II are bound to the enzyme whereas the remaining three glycine residues and the rest of lipid II probably hang outside the nucleophile binding site. Since sortase-catalyzed hydrolysis of a LPETG peptide in the absence of triglycine is slow, we speculate that hydrolysis of a LPETG motif-containing surface protein might also be slow unless lipid II, the receptor nucleophile, becomes available. This mechanism may be important for reducing wasteful escape of the surface protein from cell wall attachment. The close association of sortase and its substrates near the cell membrane may provide additional mechanisms for regulation of this type of cell wall sorting reaction.

SUMMARY

We have investigated the in vitro steady-state kinetic behaviors of *S. aureus* sortase using a LPETG peptide. The transpeptidation reaction follows a ping-pong mechanism, in which the nucleophile only binds to an acyl-enzyme intermediate. The results fully support the formation of a common acyl-enzyme intermediate in transpeptidation and hydrolysis in the absence of a nucleophile. These two reactions have a distinct rate-limiting step: the acylation step in transpeptidation and the deacylation in hydrolysis. The present kinetic analysis of sortase has now provided a solid basis for the biochemical characterization of sortase inhibitors. We have also demonstrated in this study that the nucleophile binding site of *S. aureus* sortase is specific for diglycine. While S1′ and S2′ sites both prefer glycine, the S1′ site only accommodates a glycine residue. Since sortase from certain Gram-positive bacteria has a distinct preference for the nucleophile (*19*), broad spectrum sortase inhibitors targeting the LPET site, not the leaving group/nucleophile site, are most desired.

ACKNOWLEDGMENT

The authors thank Guixian Jin, Cynthia Kenny, Girija Krishnamurthy, and Mei-Chu Lo for critical comments of the manuscript.

APPENDIX

Derivation of Steady-State Kinetic Equations for Hydrolysis and Transpeptidation Reactions As Depicted in Scheme 1. (a) Hydrolysis. We first define S_1 and $K_m^{\circ}{}_{Pep}$:

$$S_1 = [\text{peptide}] \tag{1′}$$

$$K_m^{\circ}{}_{Pep} = \frac{k_2 + k_{-1}}{k_1} \tag{2′}$$

Net rate constants as defined by Cleland (*16*) for the third, second, and first steps can be expressed as

$$k_3' = k_4 \tag{3′}$$

$$k_2' = k_2 \tag{4′}$$

$$k_1' = k_1 S_1 \frac{k_2}{k_2 + k_{-1}} \tag{5′}$$

The reaction rate (v) is inversely proportional to the sum of reciprocals of $k_1′$, $k_2′$, and $k_3′$ (*16*):

$$v = \frac{E_t}{\frac{1}{k_1'} + \frac{1}{k_2'} + \frac{1}{k_3'}} \tag{6′}$$

Substitution of eqs 3′, 4′, and 5′ into eq 6′ yields eq 7′:

$$v = \frac{E_t \frac{k_2 k_4}{k_2 + k_4} S_1}{S_1 + \frac{k_2 + k_{-1}}{k_1} \frac{k_4}{k_2 + k_4}} \tag{7′}$$

Therefore

$$k_{cat} = \frac{k_2 k_4}{k_2 + k_4} \tag{8′}$$

$$K_m = K_m^{\circ}{}_{Pep} \frac{k_4}{k_2 + k_4} \tag{9′}$$

(b) Transpeptidation. We first define S_1, S_2, $K_m^{\circ}{}_{Pep}$, and $K_m^{\circ}{}_{Nu}$:

$$S_1 = [\text{peptide}] \tag{1′}$$

$$S_2 = [\text{nucleophile}] \tag{10′}$$

$$K_m^{\circ}{}_{Pep} = \frac{k_2 + k_{-1}}{k_1} \tag{2′}$$

$$K_m^{\circ}{}_{Nu} = \frac{k_5 + k_{-3}}{k_3} \tag{11′}$$

Net rate constants as defined by Cleland (*16*) for the fourth, third, second, and first steps can be expressed as

$$k_4' = k_5 \tag{12′}$$

$$k_3' = k_3 S_2 \frac{k_5}{k_5 + k_{-3}} \tag{13′}$$

$$k_2' = k_2 \tag{14′}$$

$$k_1' = k_1 S_1 \frac{k_2}{k_2 + k_{-1}} \tag{15′}$$

The reaction rate (v) is inversely proportional to the sum of the reciprocals of $k_1′$, $k_2′$, $k_3′$, and $k_4′$ (*16*):

$$v = \frac{E_t}{\frac{1}{k_1'} + \frac{1}{k_2'} + \frac{1}{k_3'} + \frac{1}{k_4'}} \tag{16′}$$

Substitution of eqs 12′, 13′, 14′, and 15′ into eq 16′ yields eq 17′:

$$v = \frac{E_t S_1 k_2 \dfrac{\dfrac{k_5}{1 + \dfrac{k_5 + k_{-3}}{k_3 S_2}}}{k_2 + \dfrac{k_5}{1 + \dfrac{k_5 + k_{-3}}{k_3 S_2}}}}{S_1 + \dfrac{k_2 + k_{-1}}{k_1} \dfrac{\dfrac{k_5}{1 + \dfrac{k_5 + k_{-3}}{k_3 S_2}}}{k_2 + \dfrac{k_5}{1 + \dfrac{k_5 + k_{-3}}{k_3 S_2}}}} \qquad (17')$$

Therefore, if the peptide concentration is varied while the nucleophile concentration is fixed at S_2, the experimentally determined apparent K_m for the peptide and the apparent k_{cat} are related to the microscopic constants as in eqs 18′ and 19′, respectively:

$$K_{mPep,app} = K_m^{\circ}{}_{Pep} \frac{\dfrac{k_5}{1 + K_m^{\circ}{}_{Nu}/S_2}}{k_2 + \dfrac{k_5}{1 + K_m^{\circ}{}_{Nu}/S_2}} \qquad (18')$$

$$k_{catPep,app} = k_2 \frac{\dfrac{k_5}{1 + K_m^{\circ}{}_{Nu}/S_2}}{k_2 + \dfrac{k_5}{1 + K_m^{\circ}{}_{Nu}/S_2}} \qquad (19')$$

Similarly, if the nucleophile concentration is varied while the peptide concentration is fixed at S_1, the apparent K_m for the nucleophile and the apparent k_{cat} can be expressed as eqs 20′ and 21′, respectively:

$$K_{mNu,app} = K_m^{\circ}{}_{Nu} \frac{\dfrac{k_2}{1 + K_m^{\circ}{}_{Pep}/S_1}}{k_5 + \dfrac{k_2}{1 + K_m^{\circ}{}_{Pep}/S_1}} \qquad (20')$$

$$k_{catNu,app} = k_5 \frac{\dfrac{k_2}{1 + K_m^{\circ}{}_{Pep}/S_1}}{k_5 + \dfrac{k_2}{1 + K_m^{\circ}{}_{Pep}/S_1}} \qquad (21')$$

The transpeptidation as depicted by Scheme 1 is a ping-pong bi-bi reaction. According to Segal (*20*) the ping-pong bi-bi reaction in the absence of product inhibition can be described by eqs 22′ and 23′:

$$v = \frac{V_m S_1 S_2}{K_{mNu} S_1 + K_{mPep} S_2 + S_1 S_2} \qquad (22')$$

$$v = \frac{k_1 k_2 k_3 k_5 E_t S_1 S_2}{k_1 k_2 (k_{-3} + k_5) S_1 + k_3 k_5 (k_2 + k_{-1}) S_2 + k_1 k_3 (k_2 + k_5) S_1 S_2} \qquad (23')$$

A rearrangement of eq 23′ yields eq 24′:

$$v = \frac{\dfrac{k_2 k_5}{k_2 + k_5} E_t S_1 S_2}{\dfrac{k_{-3} + k_5}{k_3} \dfrac{k_2}{k_2 + k_5} S_1 + \dfrac{k_2 + k_{-1}}{k_1} \dfrac{k_5}{k_2 + k_5} S_2 + S_1 S_2} \qquad (24')$$

Therefore

$$K_{mNu} = K_m^{\circ}{}_{Nu} \frac{k_2}{k_2 + k_5} \qquad (25')$$

$$K_{mPep} = K_m^{\circ}{}_{Pep} \frac{k_5}{k_2 + k_5} \qquad (26')$$

It now becomes clear that when $K_{mPep,app}$ and $K_{mNu,app}$ in eqs 18′ and 20′ are determined in the presence of a fixed saturating concentration of the second substrate, they become respectively equal to K_{mPep} and K_{mNu}, the Michaelis constants defined in eq 22′. It is worthwhile to note that while this statement is true in any ping-pong bi-bi reaction, it is not generally applicable to all mechanisms.

REFERENCES

1. Cossart, P., and Lecuit, M. (1998) *EMBO J. 17*, 3797−3806.
2. Navarre, W. W., and Schneewind, O. (1999) *Microbiol. Mol. Biol. Rev. 63*, 174−229.
3. Fischetti, V. A., Pancholi, V., and Schneewind, O. (1990) *Mol. Microbiol. 4*, 1603−1605.
4. Schneewind, O., Mihaylova-Petkov, D., and Model, P. (1993) *EMBO J. 12*, 4803−4811.
5. Schneewind, O., Model, P., and Pishetti, V. A. (1992) *Cell 70*, 267−281.
6. Ton-That, H., Mazmanian, S. K., Alksne, L., and Schneewind, O. (2002) *J. Biol. Chem. 277*, 7447−7452.
7. Mazmanian, S. K., Liu, G., Ton-That, H., and Schneewind, O. (1999) *Science 285*, 760−763.
8. Ton-That, H., Liu, G., Mazmanian, S. K., Faull, K. F., and Schneewind, O. (1999) *Proc. Natl. Acad. Sci. U.S.A. 96*, 12424−12429.
9. Perry, A. M., Ton-That, H., Mazmanian, S. K., and Schneewind, O. (2002) *J. Biol. Chem. 277*, 16241−16248.
10. Ruzin, A., Severin, A., Ritacco, F., Tabei, K., Singh, G., Bradford, P. A., Siegel, M. M., Projan, S. J., and Schlaes, D. M. (2002) *J. Bacteriol. 184*, 2141−2147.
11. Pallen, M. J., Lam, A. C., Antonio, M., and Dunbar, K. (2001) *Trends Microbiol. 9*, 97−101.
12. Mazmanian, S. K., Liu, G., Jenson, E. R., Lenoy, E., and Schneewind, O. (2000) *Proc. Natl. Acad. Sci. U.S.A. 97*, 5510−5515.
13. Jonsson, I.-M., Mazmanian, S. K., Schneewind, O., Verdrengh, M., Bremell, T., and Tarkowski, A. (2002) *J. Infect. Dis. 185*, 1417−1424.
14. Bierne, H., Mazmanian, S. K., Trost, M., Pucciarelli, G., Liu, G., Dehoux, P., Jansch, L., Garcia-del Portillo, F., Schneewind, O., and Cossart, P. (2002) *Mol. Microbiol. 43*, 869−881.
15. Ton-That, H., Mazmanian, S. K., Faull, K. F., and Schneewind, O. (2000) *J. Biol. Chem. 275*, 9876−9881.
16. Cleland, W. W. (1975) *Biochemistry 14*, 3220−3224.

17. Fersht, A. (1999) *Structure and Mechanism in Protein Science*, pp 132−168, W. H. Freeman, New York.
18. Ilangovan, U., Ton-That, H., Iwahara, J., Schneewind, O., and Clubb, R. T. (2001) *Proc. Natl. Acad. Sci. U.S.A. 98*, 6056−6061.
19. Dhar, G., Faull, K. F., and Schneewind, O. (2000) *Biochemistry 39*, 3725−3733.
20. Segal, I. H. (1975) *Enzyme Kinetics: Behavior and Analysis of Rapid Equilibrium and Steady-State Enzyme Systems*, pp 606−625, John Wiley and Sons, New York.

BI034391G